CI&CEQ
Chemical Industry & Chemical Engineering Quarterly

Available on line at
Association of the Chemical Engineers of Serbia *AChE*
www.ache.org.rs/CICEQ

Chem. Ind. Chem. Eng. Q. 27 (1) 35–44 (2021) CI&CEQ

MAJED M. ALGHAMDI[1]
ADEL A. EL-ZAHHAR[1,2]

[1]Environmental Monitoring, Assessment & Treatment (EMAT) Research Group, Department of Chemistry, College of Science, King Khalid University, Abha, Saudi Arabia
[2]Nuclear Chem. Dept. AEA, Cairo, Egypt

SCIENTIFIC PAPER

UDC 546.26-162-31:544:66:678

CELLULOSE ACETATE BUTYRATE GRAPHENE OXIDE NANOCOMPOSITE MEMBRANE: FABRICATION, CHARACTERIZATION AND PERFORMANCE

Article Highlights

- CAB/GO membrane exhibited improved properties and performance
- The results revealed an improvement of 450% in water flux
- Improved rejection of 144 and 93% for NaCl and Na_2SO_4, respectively
- Higher performance stability, thermal and antifouling properties

Abstract

In this study, the effects of graphene oxide (GO) nanosheets on the physico-chemical properties and performances of cellulose acetate butyrate (CAB) membranes were investigated. Nanocomposite membranes were fabricated using CAB and a small amount of GO in the range of 0 to 0.07 wt.%, using a conventional phase-inversion method. Membranes were characterized by different methods and their performances were tested using a dead-end filtration system. Compared with pristine CAB membrane, experimental results demonstrated an improvement in features such as hydrophilicity, permeability, salt rejection, antifouling, and stability. The results proved an increase in the porosity and pore sizes of membranes with GO addition. Furthermore, the membrane containing 0.07 wt.% of GO exhibited a low contact angle of 37° and a dramatic improvement in water flux of about 450% (from 2 to 11 L/(m^2 h)). Moreover, it demonstrated a salt rejection of 39% for NaCl and 87% for Na_2SO_4, corresponding to improvements of about 144 and 93%, respectively. Furthermore, the results revealed a higher antifouling property with an 86% improvement in flux recovery and higher stability in terms of performance and thermal properties compared to CAB.

Keywords: cellulose acetate butyrate, graphene oxide, nanocomposite, membrane, salt rejection.

Although synthetic polymer-based membranes are broadly used and have a huge market, complications associated with highly hydrophobic polymer backbones make them vulnerable to fouling [1]. In order to overcome this disadvantage, several methods have been employed to enhance fouling resistance, mostly by increasing the hydrophilicity [2–5]. Among these methods is the incorporation of different types of nanoparticles into membranes [6-10]. From this point of view, materials such as cellulose esters are known for their outstanding hydrophilicity and low fouling tendency in addition to their significant roles in industry and pharmaceutical technologies [11,12]. Consequently, they can be considered as promising in membrane technology. They also offer the benefit of biocompatibility and have a relatively low cost. However, the lack of reactive functional groups on the polymer chains limits their applications.

In order to enhance their properties, hydroxyl groups of cellulose can be chemically modified to form materials of different physical and chemical properties that could be appropriate for diverse applications [13]. To further enhance membrane performance, polymer blending is also one of the effective

Correspondence: M.M. Alghamdi, King Khalid University, College of Science, Department of Chemistry, P.O. Box 9004, Abha 61413, Saudi Arabia.
E-mail: mmalghamdi@kku.edu.sa
Paper received: 28 January, 2020
Paper revised: 28 May, 2020
Paper accepted: 19 June, 2020

https://doi.org/10.2298/CICEQ200128022A

methods that has provided a desirable way to fulfill the expectation of new polymeric materials properties. For example, the cellulose acetate (CA) membrane has often been modified by blending with other materials, such as hydrous manganese dioxide nanoparticles, GO and molybdenum disulfide to gain improved performance, such as higher flux and better selectivity [14,15]. Likewise, the blending of carboxymethyl cellulose acetate and CA also resulted in membranes with enhanced contact angles, morphology, permeability, and antifouling properties [16].

Nowadays, among the nanomaterials that have been incorporated into membranes is graphene oxide (GO). Due to its rich oxygen-containing hydrophilic functional groups, unique two-dimensional structure, large specific surface area, and good mechanical properties [17,18], this material has attracted considerable interest and has been exploited for various membrane applications. In fact, the incorporation of GO has proven to enhance membrane performance in terms of permeate flux, salt rejection, fouling properties, hydrophilicity and surface charges of membranes [19-23]. For example, improved hydrophilicity, permeability, and antifouling performances were observed by incorporating GO and PVDF [24]. Moreover, the work of Zinadini *et al.* also revealed a significant improvement in PES membrane fouling resistance and surface hydrophilicity by blending with GO [25]. Likewise, incorporation of GO has also resulted in improved PSF membrane performance [26]. In particular, the incorporation of GO within CA has been widely investigated and demonstrated outstanding properties. For example, incorporating GO and CA has been investigated recently and it has resulted in increased salt rejection, improved mechanical strength and thermal stability [27,28].

Nevertheless, there have been few reports on cellulose acetate butyrate (CAB)-based membrane applications. This might be due to CAB's low permeability and the fact that it is more hydrophobic than CA. In fact, CAB has a composition of butyryl and acetyl functional groups that can effectively develop the properties of the cellulose [29-32]. In addition, CAB matches the CA membrane in many characteristics but has additional features such as being tougher than CA, having great film formation, and demonstrating good solubility in organic solvents. However, in order to compete with other membranes, further modification of the CAB-based membrane is still required.

Based on these considerations and in addition to the fact that the CAB/GO composite membrane has not been investigated previously, this study was carried out to examine the influence of GO nanosheets on the CAB membrane's characteristics and performance and to address the feasibility of the nanocomposite membrane for application in salt separation. It is proposed that the use of GO could further facilitate interactions with polymers and salts and hence increase membrane stability and salt rejection during filtration [33]. Also, the use of GO could provide diffusion pathways for water transportation and thereby increase the overall flux rate during filtration; this is in addition to its effects on membrane reinforcement, fouling resistance, and antibacterial activity [34].

EXPERIMENTAL

Materials

Cellulose acetate butyrate (CAB), with an average molecular weight of 30000 Da and 49% butyryl, was obtained from Sigma-Aldrich and used as received without further purification. Polyvinylpyrrolidone (PVP) powder (*MW* = 25,000 g/mol), NaCl and Na_2SO_4 were purchased from Sigma-Aldrich. *N,N*-dimethylformamide (DMF) with 99.5% purity was supplied by Acros Organics. Graphene oxide (GO) nanosheets (flakes) with carbon content of 42-52% were purchased from Sigma-Aldrich and employed as inorganic nano-modifiers.

Fabrication of nanocomposite membrane

The nanocomposite membranes were fabricated by the casting-solution and the phase-inversion methods. The preparation was performed in a glass reactor by dissolving a fixed amount of CAB (20 wt.%) and PVP (1 wt.%) in DMF and stirring the polymeric solution for more than 1 h *via* a mechanical stirrer until complete dissolution (solution A). GO/formamide solution was prepared by dispersion of GO powders in formamide (30 wt.%) with different concentrations, and the solutions were sonicated for 1 h until forming homogeneous GO/formamide suspensions (solution B). The membrane casting-solutions with varied GO concentrations were prepared by mixing solution A with solution B as presented in Table 1. For better dispersion of GO, the casting-solutions were sonicated for 30 min *via* an ultrasonic bath. Next, the prepared homogeneous casting-solutions were casted onto glass plates by means of a casting knife with a constant thickness of 0.3 mm. Subsequently, the membranes were immersed into deionized water immediately without prior evaporation time. After the exchanging process of solvent and non-solvent, the membranes were reserved in a container filled with deionized water for 24 h to remove any soluble com-

ponents in the membrane structure. Afterward, the membranes were dried between two filter paper sheets at room temperature (25±2 °C) for 24 h.

Table 1. Composition of the prepared casting-solutions used for membranes fabrication; CAB wt.%: 20.00, PVP wt.%: 1.00

Membrane	GO wt. %	DMF wt. %
1	0	79.00
2	0.01	78.99
3	0.04	78.96
4	0.07	78.93

Membrane characterization

The hydrophilicity of membranes was studied via the water contact angle analysis using deionized water. Field emission scanning electron microscopy (SEM) was used for analyzing the surface morphology. Images were obtained using a Jeol Model 6360 LV SEM (USA). Fourier transform infrared (FTIR) spectra for the prepared membranes were obtained using Nicolet 6700 FT-IR from Thermo Scientific. The spectra of the samples were analyzed in the infrared (IR) region between 4000 and 400 cm^{-1}.

Membrane porosity was measured using the volume fraction process. In this process, the prepared membranes were soaked in deionized water for at least 24 h. The wet membranes were then taken out and the excess water was softly removed from the membranes' surfaces by the aid of tissue paper. After that, the wet membranes were weighed and then dried in a vacuum oven at 70 °C for 24 h and weighed again after drying. The porosity percentage of the membranes (ε) and the water uptake were determined by employing Eqs. (1) and (2), respectively [35]:

$$\varepsilon = 100\frac{W_s - W_d}{\rho_{water} A l} \tag{1}$$

$$\text{Water uptake, \%} = 100\frac{W_s - W_d}{W_d} \tag{2}$$

In these equations, W_s and W_d (g) are the weights of the swollen and dry membranes, respectively; ρ_{water} (g/cm^3) is the water density; A (cm^2) is the membrane area; and l (cm) is the membrane thickness. The membrane surface pore diameter (a) could be calculated using Eq. (3) [36]:

$$a = \sqrt{\frac{8(2.9 - 1.75\varepsilon)\mu l Q_w}{\varepsilon A \Delta P}} \tag{3}$$

where a (m) is the mean pore diameter; Q_w (m^3/s) is the volume of permeated water per unit time; A (m^2) is the membrane effective area; and l (m) is the membrane thickness. μ (Pa s) is the water viscosity at 25 °C; ΔP (Pa) is the trans-membrane pressure; and ε is the porosity percentage.

Membrane performance

The performance of the prepared membranes was investigated using a laboratory designed dead-end filtration system. The salt solutions were prepared separately by dissolving the required amount of salts (Na_2SO_4 and NaCl) in deionized water. Various concentrations of salts in the range of 1 to 2 g/L were prepared. The water flux (J_w) was acquired by determining the amount of water that passed through the membranes in terms of L/m^2 h at a fixed pressure of 1.4 bar (20 psi) and calculated using Eq. (4) [37]:

$$J_w = \frac{Q}{A\Delta t} \tag{4}$$

In Eq. (4), Q (L), A (m^2), and Δt (h) are expressed as the volume of permeated water, the membrane area, and the sampling time, respectively. For salt rejection percentage calculations, Eq. (5) was employed [37]:

$$\text{Rejection ,\%} = 100\left(1 - \frac{C_p}{C_f}\right) \tag{5}$$

where C_p and C_f are salt concentrations in permeate and feed, respectively, which were measured by a conductivity meter.

With regard to the antifouling study, the membranes were first tested using a pure water flux ($J_{w,1}$). The membranes then were subjected to the sodium alginate (SA) solution as a model of an organic fouling material. SA solution with a concentration of 20 mg/L was applied as feed solution until obtaining a stable flux. After the SA permeation experiment, the membranes were washed with deionized water and the second pure water flux ($J_{w,2}$) was then determined. The flux recovery ratio ($FR\%$) was calculated using Eq. (6), where the higher value of FR% reflects good antifouling behavior for the membranes:

$$FR\ \% = 100\left(\frac{J_{w,2}}{J_{w,1}}\right) \tag{6}$$

RESULTS AND DISCUSSION

Membrane characterization

The FTIR spectra of the CAB, GO and CAB/GO are presented in Figure 1. The spectrum of GO shows peaks at 1620, 1738 and 3420 cm^{-1} that could be assigned to C=C, C=O and OH bonds, respectively. The peak at 1050 cm^{-1} may be assigned to the epoxy group. The spectra were consistent with the literature

[38,39]. Moreover, the presence of the carboxylic acid OH can be confirmed by the broad band between 2500 and 3300 cm^{-1}.

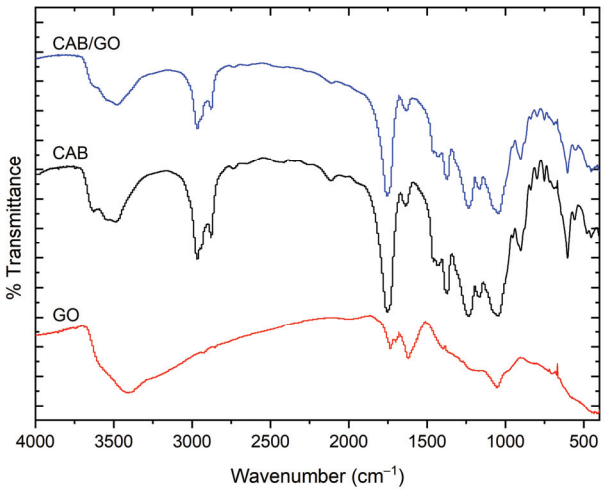

Figure 1. FTIR spectra of GO, CAB, and CAB/GO nanocomposite.

In comparison, the FTIR spectrum of CAB showed a band at 1750 cm^{-1} due to the carbonyl ester group. The peak at 1246 cm^{-1} could be assigned to the asymmetric stretching of C-C-O of the ester group; the band appeared at 1049 cm^{-1} as the result of asymmetric O-C-C stretching attached to the carbonyl carbon. The peak at 1375 cm^{-1} was due to methyl groups in acetate moiety. The absence of vibrations peaks of GO could be an indication of its complete incorporation in the polymer matrix due to its very low content [40]. Also, the overlapping of the peaks at 3630 and 3410 cm^{-1} may suggest the likely formation of hydroxyl hydrogen bonding.

With regard to thermal stability, the prepared CAB and CAB/0.07% GO composite membranes were studied by analyzing the thermal degradation of the samples. The results in Figure 2 showed that the thermal degradation of CAB occurred in three steps. The first step started between 90 and 200 °C with a weight loss of 31%, which involves the evaporation of bound water and the starting of cellulose degradation, yielding aliphatic char and volatile. The remaining two steps appeared between 240 and 450 °C with a total weight loss of 69%. These steps involve the conversion of some aliphatic char to aromatic and gaseous components [41]. The thermogram of CAB/0.07% GO shows one major step between 250 to 450 °C with a total weight loss of 94.5%. This step includes the evaporation of bonding water and thermal degradation of the cellulose skeleton. The presence of GO appeared to enhance thermal property of the CAB and delayed the thermal degradation of the cellulosic materials. This finding could be due to the increased surface area in the presence of GO, which decreased the heat release rate and mass loss rate as well. Also, the GO accumulated on the surface or within the melt polymer layer, acting as a thermal insulation layer and delaying the cellulose degradation.

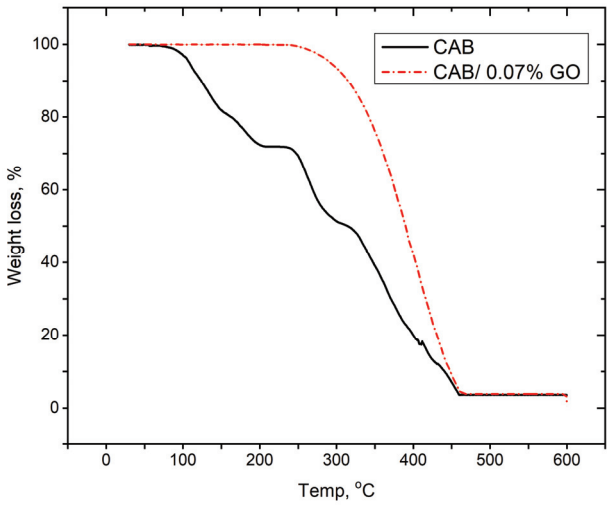

Figure 2. TGA thermograms of CAB and the prepared CAB/0.07 wt.% GO composite, under N_2 atmosphere (10 mL/min) at a heating rate of 10 °C/min.

Furthermore, the effect of GO nanosheets on the morphological surface characteristics of the membrane samples was studied using SEM (Figure 3). The SEM micrographs revealed a porous surface layer with a more sponge-like appearance than those on the CAB membrane [42]. The SEM results clearly showed that GO has a significant effect on the membrane. This could be attributed to the influence that GO, as a hydrophilic material, has on the dynamic stability of the casting solution and hence the phase-inversion process [43]. The addition of GO caused a fast phase separation during the phase-inversion process, which can also lead to higher porosity and the formation of larger pores in the membrane's surface. This outcome might be related to GO functional groups, small amount, and the carbon-based structure of the CAB polymer and GO. In addition, no agglomeration of GO nanomaterials was observed. This could be the result of better dispersion of GO particles due to their functionality, small amount, and a result of the sonication process that was used, which was set at 30 min for verifying optimal dispersion.

The membrane sample's hydrophilicity was measured by determining the contact angle using water drops on the membrane surfaces. The results in Table 2 show variations of membrane-water contact

angles at different concentrations of GO. The membrane water contact angle for CAB was found to be around 79°, which is consistent with the literature [44]. Furthermore, it was found that the contact angle significantly decreased with increasing GO concentrations, *i.e.*, the contact angle decreased from 79 to 37°. These results reflect a significant effect of GO on the hydrophilicity of membrane surfaces, even with a very small amount, improving the membranes' hydrophilicity with the GO incorporation within the range of 0 to 0.07 wt.%. This finding may be attributed to the hydrophilic nature of GO and the formation of bigger pores as well.

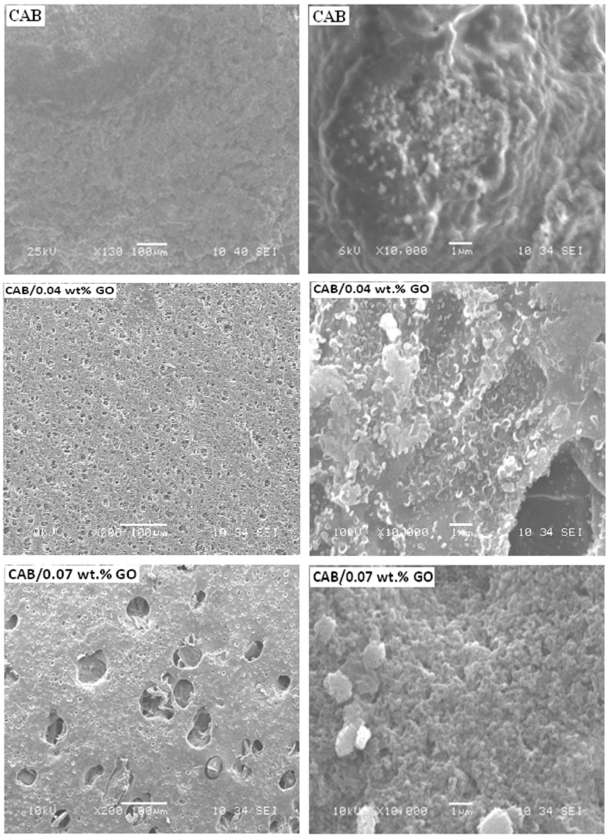

Figure 3. SEM images of: A) the pristine CAB; B) CAB/0.07 wt.% GO composite.

Table 2. CAB/GO nanocomposite membranes characterizeations; membrane thickness: 0.3 mm

GO wt.%	Contact angle °	Porosity %	Mean pore diameter nm	Water uptake %
0	79	54.3	13.4	11.2
0.01	60	65.6	25.2	15.6
0.04	53	76.7	28.3	18.5
0.07	37	84.6	32.1	22.6
0.10	47	71.7	23.12	16.7

In terms of the membranes' porosity and mean pore sizes, it is clear from the results presented in Table 2 that the porosity and mean pore diameter effectively increased with increasing GO content ratios. A small addition of 0.07 wt.% of GO resulted in a considerable increase of around 55 and 140% in porosity and mean pore diameter, respectively. For water uptake percentage, the results also displayed a significant increase in water uptake with an increasing GO content ratio. This may be attributed to the GO inclusion into the membrane surface and within the membrane body that could lead to an increase in both the -OH and -COOH hydrogen bonds, effectively enhancing the hydrophilic property of the membrane and increasing the water absorption, in agreement with the contact angle results. To the contrary, the membrane sample with 0.1 wt.% showed no significant increase in the porosity.

Though the presence of well-dispersed GO could obviously improve the morphology, porous structure and pore size, using larger amounts of GO could negatively affect the nature and type of the pores that are formed [43]. With a higher amount of GO nanomaterials (>0.07 wt.%), the membrane properties exhibited contradictory effects [26]. This might be attributed to GO's ability to migrate through the membrane layer toward the surface when the phase-inversion process take place. This could cause significant changes in the membrane's surface pores and hydrophilicity, decreasing water passage and adsorption of water on the membrane's surface [45].

Membrane performance

Water flux

The pure water flux of the prepared nanocomposite membranes was investigated. The results are shown in Figure 4. The results demonstrated an obvious increase in water flux with GO content, up to 0.07 wt.%. The membrane containing 0.07 wt.% of GO exhibited a water flux of 7.9 L/(m^2 h bar), corresponding to an improvement of about 450% in water flux. This result is comparable to what was obtained for the carbon nanotube membrane/GO [46] and the result is higher than what was found for other GO-incorporated, polymer-based membranes, as shown in Table 3. This finding could be related to the increase in membrane hydrophilicity, which is known to enhance the water flux [47], and which is in agreement with contact angle measurements. Furthermore, the increase of the water flux is consistent with SEM images and the obtained increase in porosity and pore size measurements. This enabled migration of more water molecules through the membrane layer and it imp-

roved the water flux [48,49]. It has been reported that improvements in hydrophilicity significantly enhance membrane flux as a result of the adsorption of water molecules on the membrane's surface through hydrogen bonding and/or electrostatic interactions [50]. The addition effects of GO on porosity and pore size could further influence membrane permeability. Nevertheless, any further increase in GO content could have decreased the water flux, as the high concentration of nanoparticles could have caused pore blocking, which would have hindered the water transfer [51,52]. On the other hand, bad nanoparticle dispersion or a nanoparticle agglomeration in the membrane interlayer could also have reduced water flux, which would have resulted in poor membrane performance [53].

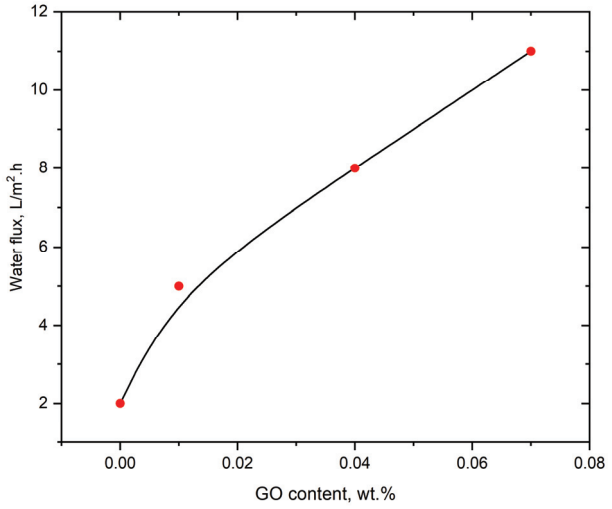

Figure 4. Effect of GO content on the water flux, carried out at a pressure of 1.4 bar.

Salt rejection

The salt rejection efficiency of the prepared membranes was investigated using NaCl and Na_2SO_4 solutions. The results (shown in Figure 5) illustrated an obvious increase in salts rejection with increasing GO content. The results demonstrated a salt rejection of 39% for NaCl and 87% for Na_2SO_4 obtained with 0.07 wt.% of GO, which corresponded to improvements of about 144 and 93% in salt rejection, respectively. Comparisons of performance with other similar GO membranes are shown in Table 3. The nanocomposite membranes of CAB/0.07 wt.% GO illustrated comparable ionic rejection results for NaCl and better results for Na_2SO_4. These results may be explained on the basis of the adsorption properties of the GO nanomaterials, which enhanced the interactions between ions and the membrane matrix, both on the surface and within the pores. Also, such behavior might be related to the possible produced surface charges, which could promote the cation exchange processes. Although this would appear to oppose the trade-off effect that existed between the flux and rejection, a similar observation was reported and proved by Ganesh *et al.* [54].

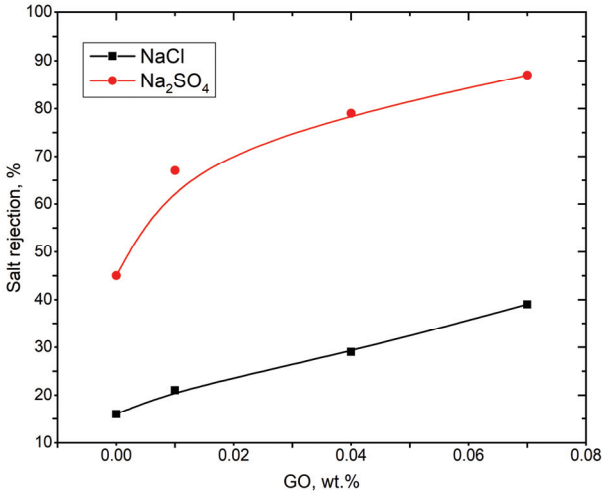

Figure 5. Effect of GO content on the salt rejection efficiency, carried out at a pressure of 1.4 bar.

Effect of permeate volume on the salt rejection

The salt rejection efficiency was also studied against the permeation volume; results are shown in Figure 6. The results clarified that the composite

Table 3. Comparison of flux and salt rejection of different GO-incorporated membranes

Membrane	Water flux, L/(m^2 h bar)	Salt rejection (1000 ppm)		Ref.
		NaCl	Na_2SO_4	
GO	4.76	59%	95.1%	[46]
Carbon nanotube / GO (1:8 mass ratio)	8.02	51.4%	80.0%	[46]
PSF / (1000ppm GO)	2.5	~ 43%	~ 65%	[54]
PSF / (2000ppm GO)	2.5	~ 58%	72%	[54]
CA / (0.005wt.%GO)	0.5	80% (2000ppm)	-	[43]
PES / (0.1wt.%GO)	3.3	-	-	[25]
CAB / (0.07wt.%GO)	7.9	39%	87%	Present work

membranes containing GO showed a higher stable salt rejection with permeate volume, reflecting a higher stability of nanocomposite membrane than the pure CAB membrane. This was observed for both NaCl and Na_2SO_4 solutions. Moreover, the results showed a slight effect on the stability of the nanocomposite membrane with 0.07 wt.% of GO than that of 0.04 wt.% GO. This observation leads to the expectation that increasing GO concentrations of more than 0.07% could provide bad dispersion within the polymeric moiety and lead to lowering the membrane stability. The results obtained regarding this concern showed that the optimal GO concentration to be used in the nanocomposite membrane is 0.07 wt.%.

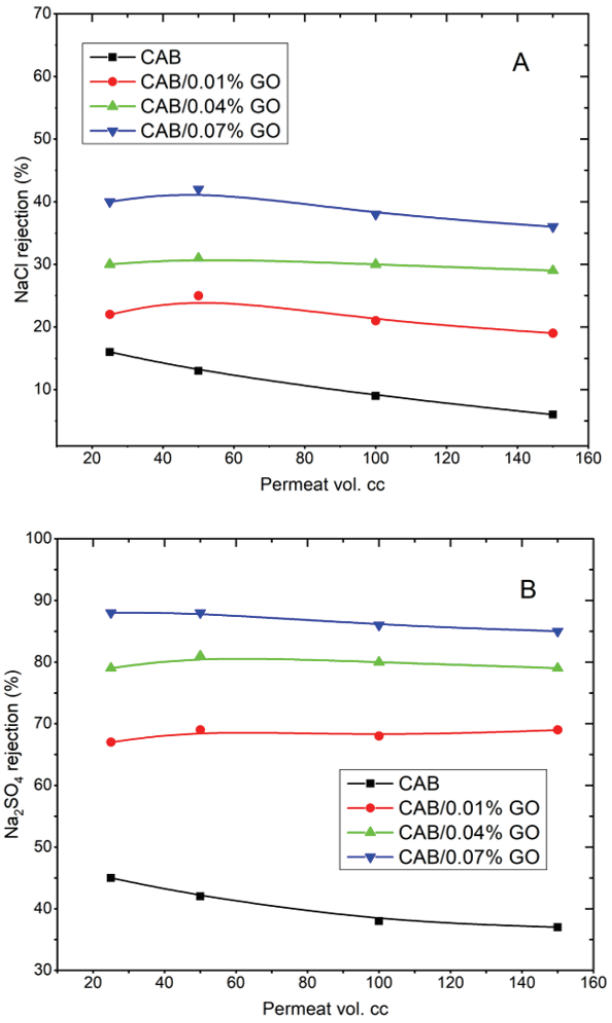

Figure 6. Effect of permeation volume on the salt rejection efficiency: A) for NaCl; B) for Na_2SO_4, using a feed concentration of 1 g/L.

Effect of feed solution concentration on membrane performance

The salt rejection and permeation flux levels of the prepared nanocomposite membranes were also studied at a range of feed concentrations up to 2 g/L. As shown in Figure 7, the results revealed that Na_2SO_4 and NaCl concentrations had a clear effect on membrane performance. A decrease in both salt rejection and permeation flux was noted as feed concentration increased. In terms of salt rejection performance (Figure 7A), a decrease in salt rejection efficiency of about 14% for Na_2SO_4 and 20% for NaCl was attained. This could be attributed to the effect of the Donnan exclusion of co-ions, which could influence the diffusion transport of ions through the membrane [55]. In addition, the effect of high concentrations on the polarization and possible weakening of electrostatic interaction between the ions in the aqueous solution and the charges on the membrane's surface may consequently lead to an increase in ions permeation and therefore decrease rejection efficiency [56].

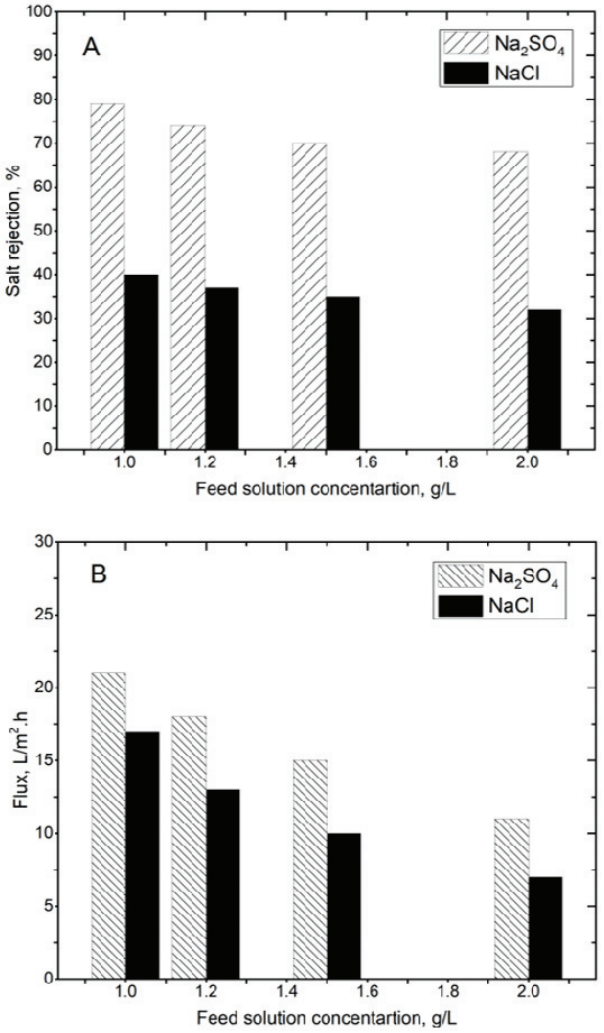

Figure 7. ffect of feed solution concentration of NaCl and Na_2SO_4 on: A) salt rejection efficiency; B) permeation flux rate employing 0.04 wt.% GO nanocomposite membrane at 2.8 bar.

Feed concentration had a more significant effect on permeation flux, with flux reduction of around 49 and 58% for Na_2SO_4 and NaCl solutions, respectively. These results could be explained as follows: as salt concentration increases, there are more ions competing to be adsorbed onto the membrane surfaces; the presence of more ions could decrease pore size and therefore decrease permeation. This finding could also be attributed to concentration polarization, where a denser boundary layer may lead to a decrease in water flux. In addition to the polarization effect, in a high electrolytic solution, the membrane material could shrink and pore size could decrease, causing flux to decrease when feed concentration is higher [57,58].

Antifouling study

The fouling could be considered as the formation of a gel-like layer on the membrane surface as a result of adsorption or the deposition of organic matter within the pores or the surface of the membrane. The improvement of antifouling behavior of the membrane depends on the membrane's hydrophilicity, which could be enhanced by inclusion of hydrophilic groups like –OH and/or –COOH on the membrane surface [59,60]. The CAB/GO composite membranes were highly hydrophilic when compared with pure CAB membranes due to the enhanced water affinity by the presence of GO. The increased water affinity decreased hydrophobic adsorption/deposition of SA on the nanocomposite membrane surface or within the pores. The results presented in Figure 8 represent the water flux of CAB and CAB/GO composite membranes with different GO content ratios. These results show a clear improvement in flux recovery ratio with increasing GO content ratio. This improvement could be attributed to the enhanced hydrophilicity, supported by the change in water contact angle (Table 2). In addition, the presence of GO within the membrane material could create strong electrostatic forces, creating an energetic barrier for the adsorption of SA [61]. Also, the hydroxyl/carboxyl groups of GO could interact with water molecules via Van der Waals forces and hydrogen bonding and forming a molecular layer of water on the membrane surface, which prevents the deposition and/or adsorption of SA [62]. It could be concluded that the presence of GO has an important role in improving antifouling performance of the composite membrane with content up to 0.07 wt.%.

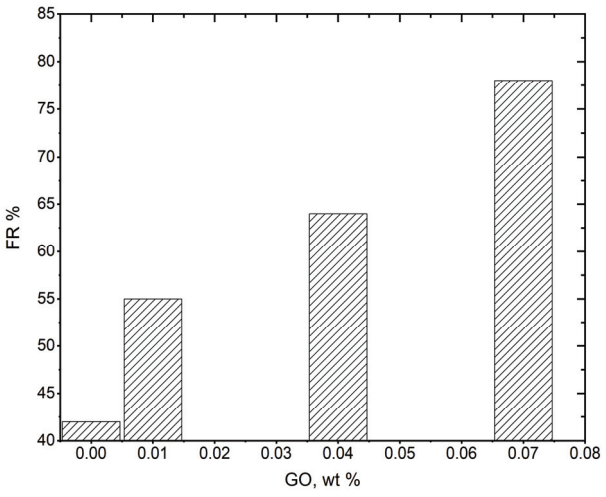

Figure 8. Effect of GO content on the flux recovery ratio of the nanocomposite membranes.

CONCLUSIONS

The results of this work demonstrated characterization and application of a new synthesized membrane nanocomposite of CAB/GO. Based on the results, the nanocomposite membrane proved its significance in terms of improvements in flux, salt rejection, fouling resistance, and stability. As compared to pristine CAB, an increase in the porosity and the pore sizes of membranes with GO content ratios were demonstrated. This resulted in a dramatic improvement in water flux of about 450%, along with 144 and 93% for NaCl and Na_2SO_4 rejection, respectively. Furthermore, the results showed high stability of the nanocomposite membrane toward feed concentration with the separation and flux rate, in addition to higher antifouling and thermal stability properties.

Nomenclature

Symbols

ε	Membrane porosity
W_s	Weight for swollen membrane
W_d	Weight for dry membrane
ρ_w	Density of water
r	Radius of membrane
Q	Volume of permeated water
l	Thickness of membrane
a	Mean pore diameter
μ	Viscosity of water
Q_w	Volume of permeated water per unit time
A	Filtration area
ΔP	Transmembrane pressure
V	Volume of permeate
t	Time interval
C_f	Concentration of the feed
C_p	Concentration of the permeate
$FR\%$	Flux recovery ratio
J_w	Pure water flux
$J_{w,1}$	Pure water flux before fouling

$J_{w,2}$ Pure water flux after fouling

Acknowledgments

The authors extend their appreciation to the Deanship of Scientific Research at King Khalid University for funding this work through the General Research Project under grant number (G.R.P-18-40)".

REFERENCES

[1] C. Güell, R.H. Davis, J. Membr. Sci. 119 (1996) 269-284

[2] A. Akthakul, R.F. Salinaro, A.M. Mayes, Macromolecules 37 (2004) 7663-7668

[3] P. Wang, K.L. Tan, E.T. Kang, K.G. Neoh, J. Adhes. Sci. Technol. 16 (2002) 111-127

[4] F. Liu, C.H. Du, B.K. Zhu, Y.Y. Xu, Polymer 48 (2007) 2910-2918

[5] A.A. El-Zahhar, M.M. Alghamdi, B.M. Asiri, Desalin. Water Treat. 155 (2019) 381-389

[6] H. Rabiee, V. Vatanpour, M.H.D.A. Farahani, H. Zarrabi, Sep. Purif. Technol. 156 (2015) 299-310

[7] V. Vatanpour, M. Esmaeili, M.H.D.A. Farahani, J. Membr. Sci. 466 (2014) 70-81

[8] V. Vatanpour, S.S. Madaeni, A.R. Khataee, E. Salehi, S. Zinadini, H.A. Monfared, Desalination 292 (2012) 19-29

[9] M.M. Alghamdi, A.A. El-Zahhar, B.M. Asiri, Desalin. Water Treat. 165 (2019) 54-62

[10] M.S. Sri Abirami Saraswathi, A. Nagendran, D. Rana, J. Mater. Chem., A 7 (2019) 8723-8745

[11] T. Shibutani, T. Kitaura, Y. Ohmukai, T. Maruyama, S. Nakatsuka, T. Watabe, H. Matsuyama, J. Membr. Sci. 376 (2011) 102-109

[12] X.Y. Qiu, S.W. Hu, Materials 6 (2013) 738-781

[13] A. Shanbhag, B. Barclay, J. Koziara, P. Shivanand, Cellulose 14 (2007) 65-71

[14] S. Vetrivel, D. Rana, M.S. Sri Abirami Saraswathi, K. Divya, N.J. Kaleekkal, A. Nagendran, Polym. Adv. Technol. 30 (2019) 1943-1950

[15] S. Vetrivel, M.S.A. Saraswathi, D. Rana, A. Nagendran, Int. J. Biol. Macromol. 107 (2018) 1607-1612

[16] B.X. Han, D.L. Zhang, Z.Q. Shao, L.L. Kong, S.Y. Lv, Desalination 311 (2013) 80-89

[17] R.K. Joshi, S. Alwarappan, M. Yoshimura, V. Sahajwalla, Y. Nishina, Appl. Mater. Today 1 (2015) 1-12

[18] R. Van Noorden, Nature 442 (2006) 228-229

[19] Y. Wei, Y. Zhang, X. Gao, Z. Ma, X. Wang, C. Gao, Carbon 139 (2018) 964-981

[20] A. Nicolaï, B.G. Sumpter, V. Meunier, Phys. Chem. Chem. Phys. 16 (2014) 8646-8654

[21] Q. Xu, H. Xu, J. Chen, Y. Lv, C. Dong, T.S. Sreeprasad, Inorg. Chem. Front. 2 (2015) 417-424

[22] J. Zhang, Z. Xu, M. Shan, B. Zhou, Y. Li, B. Li, J. Niu, X. Qian, J. Membr. Sci. 448 (2013) 81-92

[23] G.S. Lai, W.J. Lau, P.S. Goh, A.F. Ismail, N. Yusof, Y.H. Tan, Desalination 387 (2016) 14-24

[24] J. Zhang, Z. Xu, W. Mai, C. Min, B. Zhou, M. Shan, Y. Li, C. Yang, Z. Wang, X. Qian, J. Mater. Chem., A 1 (2013) 3101-3111

[25] S. Zinadini, A.A. Zinatizadeh, M. Rahimi, V. Vatanpour, H. Zangeneh, J. Membr. Sci. 453 (2014) 292-301

[26] L.M. Camacho, T.A. Pinion, S.O. Olatunji, Sep. Purif. Technol. 240 (2020) 116645

[27] S.M. Ghaseminezhad, M. Barikani, M. Salehirad, Composites, B 161 (2019) 320-327

[28] Y. Jahani, Desalin. Water Treat. 164 (2019) 62-74

[29] R.J. Lee, Z.A. Jawad, A.L. Ahmad, H.B. Chua, Process Saf. Environ. Prot. 117 (2018) 159-167

[30] P. Kunthadong, R. Molloy, P. Worajittiphon, T. Leejarkpai, N. Kaabbuathong, W. Punyodom, J. Polym. Environ. 23 (2015) 107-113

[31] A.D. Sabde, M.K. Trivedi, V. Ramachandhran, M.S. Hanra, B.M. Misra, Desalination 114 (1997) 223-232

[32] R.J. Lee, Z.A. Jawad, A.L. Ahmad, J.Q. Ngo, H.B. Chua, Improvement of CO2/N-2 separation performance by polymer matrix cellulose acetate butyrate, in: A. Saptoro, W.S. Khur, L.S. Wei, W.P.Q. Ng, M. Anwar, C. Yeo, K.E. Huey (Eds.), 29th Symposium of Malaysian Chemical Engineers, 2017

[33] P. Sun, M. Zhu, K. Wang, M. Zhong, J. Wei, D. Wu, Z. Xu, H. Zhu, ACS Nano 7 (2013) 428-437

[34] S. Liu, T.H. Zeng, M. Hofmann, E. Burcombe, J. Wei, R. Jiang, J. Kong, Y. Chen, ACS Nano 5 (2011) 6971-6980

[35] J.-F. Li, Z.-L. Xu, H. Yang, L.-Y. Yu, M. Liu, Appl. Surf. Sci. 255 (2009) 4725-4732

[36] V. Vatanpour, S.S. Madaeni, R. Moradian, S. Zinadini, B. Astinchap, Sep. Purif. Technol. 90 (2012) 69-82

[37] R. Han, S. Zhang, C. Liu, Y. Wang, X. Jian, J. Membr. Sci. 345 (2009) 5-12

[38] S. Bose, T. Kuila, M.E. Uddin, N.H. Kim, A.K.T. Lau, J.H. Lee, Polymer 51 (2010) 5921-5928

[39] X. Chang, Z. Wang, S. Quan, Y. Xu, Z. Jiang, L. Shao, Appl. Surf. Sci. 316 (2014) 537-548

[40] P. Shanmugaraj, A. Swaminathan, R.K. Ravi, M. Dasaiah, P. Senthil Kumar, A. Sakunthala, J. Mater. Sci.-Mater. Electron. 30 (2019) 20079-20087

[41] J. Alongi, G. Malucelli, Thermal Degradation of Cellulose and Cellulosic Substrates, in: Reactions and Mechanisms in Thermal Analysis of Advanced Materials, A. Tiwari, B. Raj (Eds.), Beverly, Hoboken, NJ, 2015, pp. 301-332

[42] N. Ghaemi, S.S. Madaeni, A. Alizadeh, P. Daraei, A.A. Zinatizadeh, F. Rahimpour, Sep. Purif. Technol. 85 (2012) 147-156

[43] Y. Shi, C. Li, D. He, L. Shen, N. Bao, J. Mater. Sci. 52 (2017) 13296-13306

[44] X. Fu, T. Maruyama, T. Sotani, H. Matsuyama, J. Membr. Sci. 320 (2008) 483-491

[45] P. Daraei, S.S. Madaeni, N. Ghaemi, E. Salehi, M.A. Khadivi, R. Moradian, B. Astinchap, J. Membr. Sci. 415–416 (2012) 250-259

[46] Y. Han, Y. Jiang, C. Gao, ACS Appl. Mater. Interfaces 7 (2015) 8147-8155

[47] J.-n. Shen, H.-m. Ruan, L.-g. Wu, C.-j. Gao, Chem. Eng. J. 168 (2011) 1272-1278

[48] S. Ansari, A.R. Moghadassi, S.M. Hosseini, Desalination 357 (2015) 189-196

[49] A. Gholami, A.R. Moghadassi, S.M. Hosseini, S. Shabani, F. Gholami, J. Ind. Eng. Chem. 20 (2014) 1517-1522

[50] B.S. Lalia, V. Kochkodan, R. Hashaikeh, N. Hilal, Desalination 326 (2013) 77-95

[51] C.A. Smolders, A.J. Reuvers, R.M. Boom, I.M. Wienk, J. Membr. Sci. 73 (1992) 259-275

[52] X. Chang-Fa, L. Zhao-Feng, J. Appl. Polym. Sci. 41 (1990) 439-444

[53] P. Daraei, S.S. Madaeni, N. Ghaemi, H. Ahmadi Monfared, M.A. Khadivi, Sep. Purif. Technol. 104 (2013) 32-44

[54] B.M. Ganesh, A.M. Isloor, A.F. Ismail, Desalination 313 (2013) 199-207

[55] S.L. Ong, W.W. Zhou, L.F. Song, W.J. Ng, Environ. Eng. Sci. 19 (2002) 429-439

[56] Y. He, G.-M. Li, H. Wang, Z.-W. Jiang, J.-F. Zhao, H.-X. Su, Q.-Y. Huang, J. Taiwan Inst. Chem. Eng. 40 (2009) 289-295

[57] L. Jin, W. Shi, S. Yu, X. Yi, N. Sun, C. Ma, Y. Liu, Desalination 298 (2012) 34-41

[58] L.M. Jin, S.L. Yu, W.X. Shi, X.S. Yi, N. Sun, Y.L. Ge, C. Ma, Polymer 53 (2012) 5295-5303

[59] S.S. Madaeni, N. Ghaemi, J. Membr. Sci. 303 (2007) 221-233

[60] S.S. Madaeni, S. Zinadini, V. Vatanpour, J. Membr. Sci. 380 (2011) 155-162

[61] K. Nakamura, K. Matsumoto, J. Membr. Sci. 280 (2006) 363-374

[62] V. Vatanpour, S.S. Madaeni, R. Moradian, S. Zinadini, B. Astinchap, J. Membr. Sci. 375 (2011) 284-294.

MAJED M. ALGHAMDI[1]
ADEL A. EL-ZAHHAR[1,2]

[1]Environmental Monitoring, Assessment & Treatment (EMAT) Research Group, Department of Chemistry, College of Science, King Khalid University, Abha, Saudi Arabia
[2]Nuclear Chem. Dept. AEA, Cairo, Egypt

NAUČNI RAD

NANOKOMPOZITNA MEMBRANA NA BAZI CELULOZNOG ACETO-BUTIRATA I GRAFEN-OKSIDA: IZRADA, KARAKTERIZACIJA I PERFORMANSE

U ovoj radu, istraživani su efekti nanopropusnih listova grafen oksida (GO) na fizičko-hemijska svojstva i performanse membrana na bazi celuloznog aceto-butirata (CAB). Nanokompozitne membrane su proizvedene korišćenjem CAB i male količine GO u opsegu 0-0,07% primenom konvencionalne metode fazne inverzije. Membrane su okarakterisane različitim metodama, a njihove performanse su testirane pomoću sistema za filtraciju sa proticanjem normalno na membranu. U poređenju sa tradicionalnom CAB membranom, eksperimentalni rezultati su pokazali poboljšanje karakteristika, kao što su hidrofilnost, propustljivost, izdvajanje soli, protiv-obrastanje i stabilnost. Rezultati su dokazali povećanje poroznosti i veličine pora membrana uz dodatak GO. Dalje, membrana koja sadrži 0,07% GO pokazala je nizak kontaktni ugao od 37° i dramatično poboljšanje vodenog fluksa od oko 450% (od 2 do 11 L/(m^2/h)). Štaviše, pokazalo je izbacivanje soli od 39% za NaCl i 87% za Na_2SO_4, što odgovara poboljšanjima od oko 144, odnosno 93%. Dalje, rezultati su pokazali veće svojstvo protiv-obrastanja sa 86% poboljšanjem fluksa i većom stabilnošću u pogledu performansi i termičkih svojstava u poređenju sa CAB.

Ključne reči: celulozni acetate-butirat, grafen-oksid, nanokompozit, membrana, izdvajanje soli.